Check for updates

Original Article

Institution of MECHANICAL ENGINEERS

Journal of ENGINEERING MANUFACTURE

Proc IMechE Part B:
J Engineering Manufacture
1–9
© IMechE 2025
Article reuse guidelines:
sagepub.com/journals-permissions
DOI: 10.1177/09544054251344686
journals.sagepub.com/home/pib
Sage

Influence of graphite nodules on the wear resistance of nodular cast iron in reciprocal sliding against deep-drawing Interstitial-Free (IF) steel

Sergio L Manenti[1], Steffen A da C Aichholz[1], Carlos AH Laurindo[1], Paulo Soares[1], Chetan P Nikhare[2], Paulo VP Marcondes[3] and Ricardo D Torres[1]

Abstract

Nodular cast iron stamping dies are extensively applied in the automotive industry to manufacture low carbon steel bodywork components. During the process, a flat steel plate is typically stamped by deep drawing in a defined die shape, causing wear to the entry radius of the nodular cast iron die. Although the graphite nodules present in the die microstructure are indicated to improve wear resistance due to its solid lubricant capability, few studies have investigated how the microstructure characteristics affect die wear. Therefore, this study investigates the influence of the number, size, as well amount of pearlite and ferrite in the wear resistance of a nodular cast iron in reciprocal sliding against a commercial Interstitial-Free (IF) deep-drawing steel. The reciprocal sliding tribology tests were conducted according to ASTM G133-05 standard in a ball-on-flat configuration. The nodular cast iron pins were extracted from a round bar obtained by FUCO® continuous casting in three different radial positions, which produces pins with distinct microstructures. A commercial zinc-aluminum coated flat IF steel plate was selected as the counter body. The coefficient of friction and wear rate were accessed for the three tribo-pair configurations. Also, the pin's microstructure and hardness were evaluated by means of Scanning Electron Microscopy (SEM) and Brinell hardness, respectively. The results reveal that the volume of graphite nodules is constant; it reduces the friction coefficient while not interfering with the wear rate of the pins extracted from the three different positions of the FUCO bar. The wear rate is abrasive followed by oxidative wear. The most wear resistant nodular casting iron pin was the one from the surface, which presented the smallest amount of pearlite.

Keywords

Nodular cast iron, tribology, wear mechanism

Date received: 11 June 2024; accepted: 3 May 2025

Introduction

Steel sheets used during the metal forming are initially laminated and classified mainly by mechanical strength and elongation. Currently, the automotive industry is focusing on maintaining or increasing the mechanical resistance of steel plates, reducing the thickness to reduce body weight without risking safety and, at the same time, reducing environmentally harmful effluents. However, during the sheet-metal forming operations in high-volume production, the interaction between the sheet metal and the die plays a very important role in the performance of the whole forming operation. Therefore, a direct relationship can be established between the improvement and technological advances of the steel plates, directly impacting the die material,

[1]Department of Mechanical Engineering, Polytechnic School, Pontificia Universidad Católica do Paraná, Curitiba, Paraná, Brazil
[2]Mechanical Engineering Department, The Behrend College, The Pennsylvania State University, Erie, PA, USA
[3]Department of Mechanical Engineering, Technology Sector, Federal University of Paraná, Curitiba, Paraná, Brazil

Corresponding author:
Chetan P Nikhare, Mechanical Engineering Department, The Behrend College, The Pennsylvania State University, 5101 Jordan Road, Erie, PA 16563, USA.
Email: cpn10@psu.edu

making it necessary to use high-performance materials for the dies to support a production cycle.[1] When the mechanical strength of the sheet metal is improved, consequently hardness increases and elongation decreases, hindering the formability, and so causing the increase of wear on the die during the sliding of the steel plate in the matrix.[2] Therefore, tribological studies[3,4] are effective and necessary to evaluate and define an appropriate selection criterion for the material applied in the manufacturing of dies.[5,6]

Usually, the forming tools used in the deep drawing processes are fabricated of nodular cast iron due to its good mechanical properties and mainly by the lubricating effect of the graphite contained in its metal matrix.[7,8] However, the microstructure of cast iron can be constituted of a ferritic matrix, which has a resistance limit value of 380–450 MPa, combined with stretching values between 10% and 22%.[9] In contrast, in nodular cast irons with a pearlitic matrix, the resistance limit can reach up to 900 MPa, with elongation around 2%.[10] Ductility is an important property of this material, consequently, due to its excellent combination of properties, it is possible to adapt it to several tribological applications.[11,12] The amount and distribution of nodules are two factors that influence the mechanical properties of nodular cast iron. In pearlitic nodular cast iron, a high number of nodules increases the tensile strength; however, for a ferritic nodular cast iron, a high number of nodules increases the elongation.[9] The size of nodules and the spacing between them have a direct relationship with the nodules count in the metal matrix; this means a high number of nodules is usually associated with smaller nodules. The cooling rate during solidification, inoculation and chemical composition influences the size of nodules. High carbon and silicon contents tend to form larger nodules, as well as slower solidification rates (thick pieces), and a more efficient inoculation tends to form smaller nodules.[9] Study of V-alloyed nodular cast iron by varying the V concentration shows that higher than 0.5 wt% V increases the wear.[13] Addition of Sn shows the increase in nodular graphite by initiating the ferrite to pearlite transformation. However, this created the low strength matrix which increased the wear in the form of spalling and delamination.[14] With surface and heat treatment processes nodular cast iron hardenability and diffusion ability can be controlled.[15] It shows that induction surface hardening decreases the abrasive wear. Nodular level and area fraction of carbides in the nodular cast iron with random pearlite-ferrite matrix shows higher hardness.[16]

The forming die wear is one of the main factors to determine the tool life in the automotive industry. The dies must withstand the main stresses of the sheet during the forming process and the sliding pressure between the surfaces.[17] A long-lasting tool life is economically interesting, as it decreases overall costs and presses down the production time. After several press strokes, wear occurs in the die, causing imperfections such as galling and scratching. The question to be addressed is: What specific factors can be optimized in the production process of nodular cast iron to enhance its wear resistance? How does the wear behavior of nodular cast iron compare to other materials commonly used in die manufacturing? What are the long-term effects of different surface coatings on the performance and longevity of forming dies? When the tool wear exceeds a certain tolerated level, the production process must stop, and the tool needs to be refurbished.[18–20]

Currently, various coatings have been applied to nodular cast iron to reduce wear, including laser cladding, Plasma Transferred Arc Alloying (PTA),[21] Physical Vapor Deposition (PVD),[22] and hard chromium plating. However, all coatings create a barrier over the graphite, which neutralizes its lubricating effect. Therefore, this study aims to evaluate the microstructure of nodular cast iron and investigate the impact of the graphite nodules. Specifically, considering factors such as the size, number, spacing between the nodules, and the relative amounts of ferrite and pearlite, all of which influence wear resistance to some extent.[23,24]

In order to evaluate the influence of the microstructural features on the wear resistance of nodular cast iron, the wear behavior was probed by carrying out a reciprocal sliding test between nodular cast iron pins against commercial deep-drawing Interstitial-Free (IF) steel plates.

Materials and methods

Pins material and production

The nodular cast iron pins were extracted from a 120 mm diameter bar, which was obtained by the FUCO® continuous casting process. As can be seen in Figure 1(a), the pins were machined out of 120 mm diameter cross-section of the bar from three different positions: surface(S), half radius (HR) and center (C). For each position, two symmetrical pins, 20 mm in length and 6 mm in diameter were manufactured (Figure 1(b)). The pins were sequentially ground up to 1500 grit SiC paper, polished using Diamond paste (1–2 μm) and then washed and dried.

Microstructural characterization

The characteristics of nodular cast iron, including the amounts of ferrite and pearlite, the degree of nodularity, and the number of nodules per unit area, were determined according to ASTM A247-67. This analysis was conducted using an optical microscope in conjunction with image processing software (Olympus Analysis). A TESCAN-VEGA3 scanning electron microscope (SEM) was employed to examine the worn surface of the pins and the wear track on the IF steel plates. The elemental composition of the worn pins was

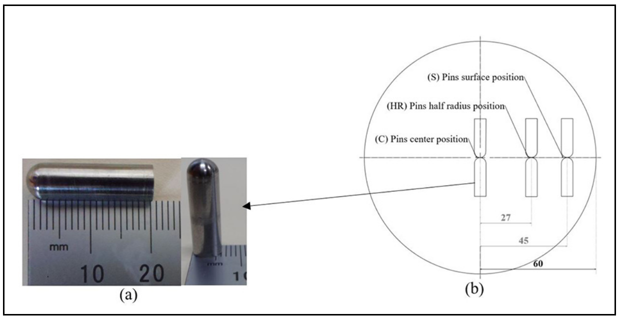

Figure 1. (a) Cross section of the bar and the location from where each pin was manufactured (surface, half radius, and center position), and (b) pins dimensions (Ø6 mm × 20 mm).

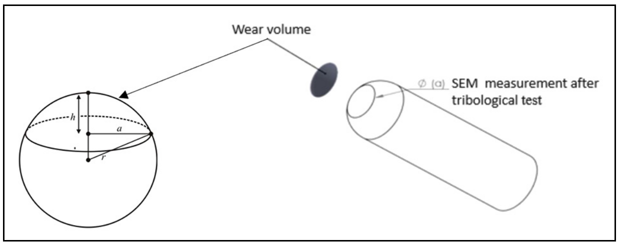

Figure 2. Schematic drawing of the worn shell of the pin, showing how the measurements were made to determine the amount of removed material.

characterized using Energy Dispersive Spectroscopy (EDS) with an Oxford microprobe.

Hardness

The evaluation of nodular casting iron hardness was conducted using a Heckert (German Democratic Republic) Brinell hardness durometer applying a load of 187.5 kgf in a 2.5 mm 100Cr6 steel indenter (HBS2.5/187.5) according to the NBR 6394-80 standard.

Tribology

The reciprocal sliding tribology tests were conducted according to ASTM G133-05 in a CSM Instruments tribometer, applying a load of 2 N over a 10 m distance with 0.5 cm/s speed. As a counter body for the pins (described in Section "Pins material and production"), a Hot dip galvanized zinc-aluminum coated steel plate (IF −DX56D + Z, + ZA) was chosen for its versatility and broad application in the manufacture of external and internal parts of automotive bodies, and commonly stamped on nodular cast iron dies. The IF steel is classified according to DIN EN 10142 and DIN EN 10327. The mechanical properties of this steel are presented in Table 1.

The steel plate was supplied by ArcelorMittal®, with a thickness of 0.75 mm, all sheets were cut in the lamination direction with dimensions of 30 mm × 25 mm.

The pins were sequentially grinded up to 1500 grit SiC paper, polished using Diamond paste (1–2 μm), simulating the actual stamping die finish used in automotive industry. Prior to and after each assay the pins were ultrasonically cleaned in deionized water for 5 min. For each position (surface, half radius, and center), two tests were performed with a normal load of 2 N, an amplitude of 2 mm, a velocity of 0.5 cm/s, and a total distance of 10 m.

Wear rate

The amount of material removed after each test was determined by the mathematical equations (1) and (2), as a function of a worn shell, as shown in Figure 2. The dimension "a" in equation (1) was measured after the completion of each test using a TESCAN-VEGA3 scanning electron microscope (SEM). Then the wear rate was calculated according to equation (3).

$$h = r - \left(\sqrt{r^2} - a^2\right) \tag{1}$$

$$V = \frac{1}{3}\pi h^2(3r - h) \tag{2}$$

$$WR = \frac{V}{LP} \tag{3}$$

Where,
V = wear volume (mm^3);
a = worn shell radius (mm);
r = pin radius (mm);
h = worn shell height (mm);
WR = wear rate (mm^3/mN);
L = sliding distance (m); and
P = normal load (N).

Results and discussion

Surface and microstructural characterization

The formation of graphite in nodular cast iron is primarily influenced by the cooling rate during solidification. This cooling rate affects the time available for carbon diffusion to occur during the eutectic reaction,

Table 1. Mechanical properties of the Deep Drawing Steel Interstitial Free (IF) DX56D + Z, + ZA.

Yield strength R_e (Mpa)	Tensile strength R_m (MPa)	Elogation A_{80} (%)	Anisotropy (r)	Strain hardening exponent (n)
120–180	260–350	⩾39	⩾1.9	⩾0.21

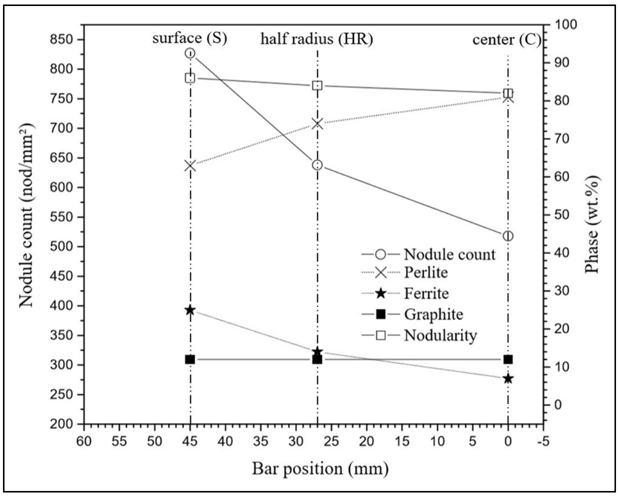

Figure 3. Results of the microstructural characterization of the bar in three different positions, surface, half radius, and center.

which ultimately determines the number of nodules per unit area, the size of the nodules, and the spacing between them. Additionally, the metallic matrix forms as the austenite cools below the eutectoid temperature.

The results in Figure 3 show the number of nodules per mm^2, as well as the percentage of pearlite, ferrite, graphite and degree of nodularity for each position: surface, half radius and center of the FUCO bar. Moreover, the horizontal axis has a scale from -5 to 60 mm is the radius of the bar, where the position 0 mm is the center (C), 27 mm is the half radius (HR), and 45 mm is the surface (S) position. On the left vertical axis is the nodule count (quantity of nodule/mm^2), while on the right vertical axis is the pearlite, ferrite, and graphite in weight percent. Also, the nodularity of the graphite nodules is plotted in the right axis of Figure 3.

According to Figure 3, the percentage of graphite remains nearly constant at 12% across all three positions in the FUCO bar. This uniformity is due to the highest count of graphite nodules at the surface (S), which is offset by their smaller size resulting from the fast-cooling rate at the surface. In contrast, the nodules are larger at the center of the FUCO bar, where the cooling rate is slower. In terms of pearlite distribution, it comprises 63% at the surface position (S), 74% at the half-radius position (HR), and 81% at the center position (C). Conversely, the percentage of ferrite decreases from 25% at the surface (S) to 14% at the half-radius (HR), and further drops to 7% at the center (C). Both microstructural features are controlled by the cooling rate of the austenite through the eutectoid temperature; fast-cooling results in a pearlite matrix while a slow cooling results in a ferritic matrix. The degree of nodularity is above 80% in all positions (C, HR, and S) indicating a nodular cast iron.

The concentration of graphite nodules at three different positions is illustrated in Figure 4. The count of nodules is recorded as 827, 638, and 518 nodules per mm^2 at the surface, half radius, and center of the FUCO bar, respectively. Figure 5(a) represents the measurements of nodules diameter obtained using a scanning electron microscope (SEM). The average diameter of the graphite nodules is 32.61 μm at the surface (S), 44.76 μm at the half radius (HR), and 55.37 μm at the center (C). According to Figure 5(b), the average distance between two adjacent nodules is 125.34 μm at the surface (S), 171.40 μm at the half radius (HR), and 208.48 μm at the center (C). Figure 5(c) plots the ratio of the distance between nodules to their diameter (L/D); it shows a consistent value of 3.6 across all three positions. Figure 5(d) illustrates the trend of hardness with position in the FUCO bar; hardness increases as one moves from the surface to the center, displaying a strong correlation with the amount of pearlite present in the microstructure. The wear behavior of nodular cast iron is influenced by multiple factors, including the ferrite/pearlite ratio, hardness, and characteristics of the graphite nodules such as their distribution, size, and, consequently, the L/D ratio.

Tribological behavior

The coefficient of friction (COF) as a function of the sliding distance for the three positions of the FUCO bar is shown in Figure 6. During the tribological tests,

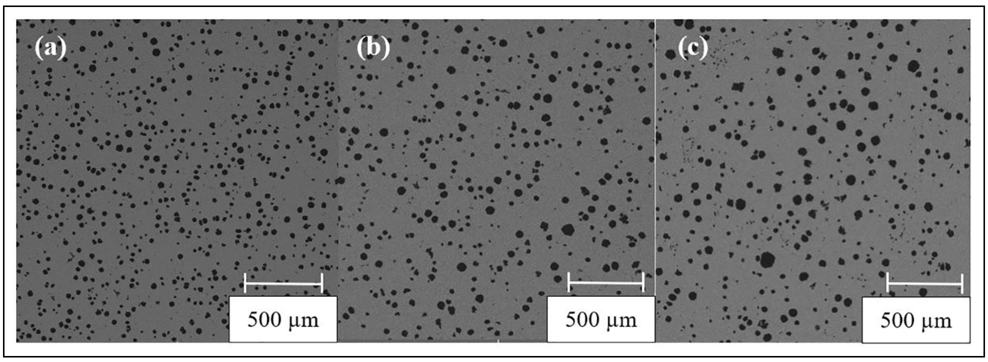

Figure 4. Optical micrograph showing the microstructure of the nodular cast iron in: (a) surface position (827 nod/mm^2), (b) half radius position (638 nod/mm^2), and (c) center position (518 nod/mm^2).

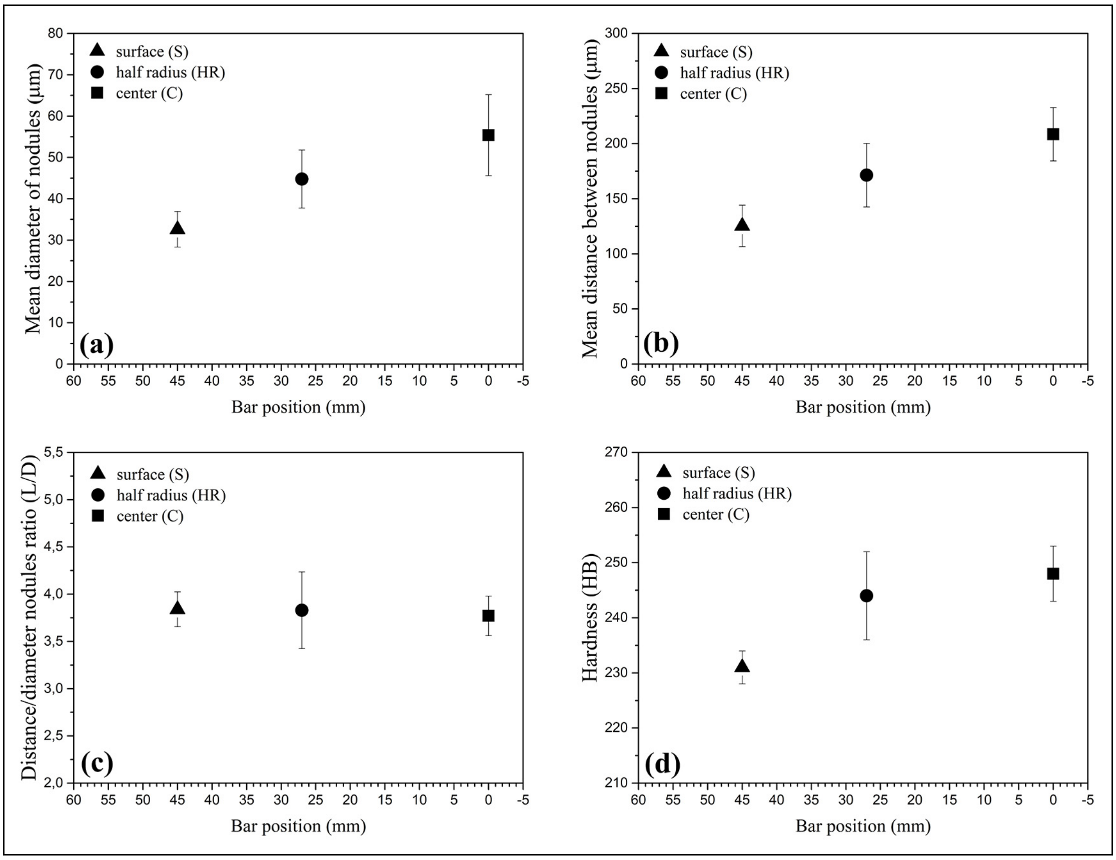

Figure 5. Influence of solidification of the cast iron bar nodular position S, HR, and C: (a) size of the nodules, (b) spacing between the nodules, (c) distance/diameter nodule ratio (L/D), and (d) hardness variation.

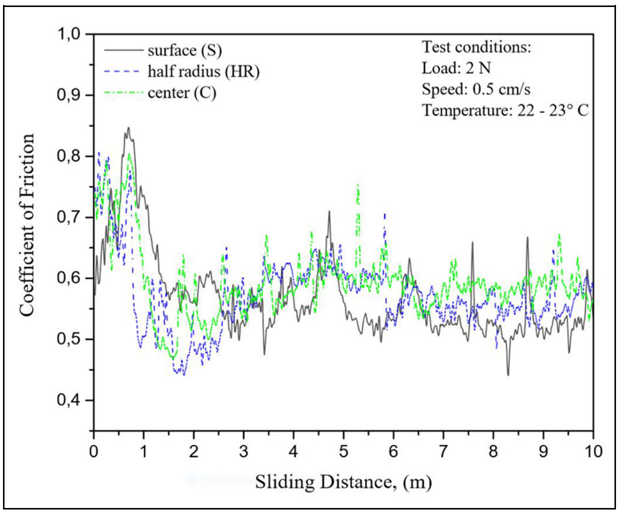

Figure 6. Coefficient of friction for each position: surface (S), half radius (HR), and center (C).

an increase in the coefficient of friction up to a mean value of 0.85 was observed, which is the running-in period. After the running-in, a reduction in the COF occurs due to the breakdown of the surface asperities of the IF plate of zinc-aluminum coating, decreasing to an average value of 0.55 in the three positions along the test. The behavior of COF between the three positions is similar and can be explained due to the same volume of graphite phase in the pins and L/D ratio. The graphite nodules are distributed differently in terms of quantity, size, and spacing in the three positions, which is influenced by the cooling rate during solidification but maintains a constant ratio between the diameter and the spacing of the graphite nodules (L/D) as observed in Figure 5(c), which keeps the volume of graphite on the pins uniform and, consequently, maintains the coefficient of friction without significant differences between the three positions during the reciprocal tribological tests. The spikes observed in the COF curve are likely related to the microstructural heterogeneous nature of nodular cast iron, which is comprised of pearlite, ferrite and graphite nodules. Additionally, the nodular cast iron pins experience a relative displacement in relation to the IF steel; it encounters soft phases, such as ferrite and graphite nodules, which are easy-to-shear phases, giving rise to the low friction coefficient, while pearlite is the harder phase, making the shear process difficult, increasing the friction coefficient, and producing spikes in COF behavior curve.

Wear behavior

Figures 7(a), 8(a), and 9(a) illustrate the wear tracks on the IF steel plate, while Figures 7(b), 8(b), and 9(b)

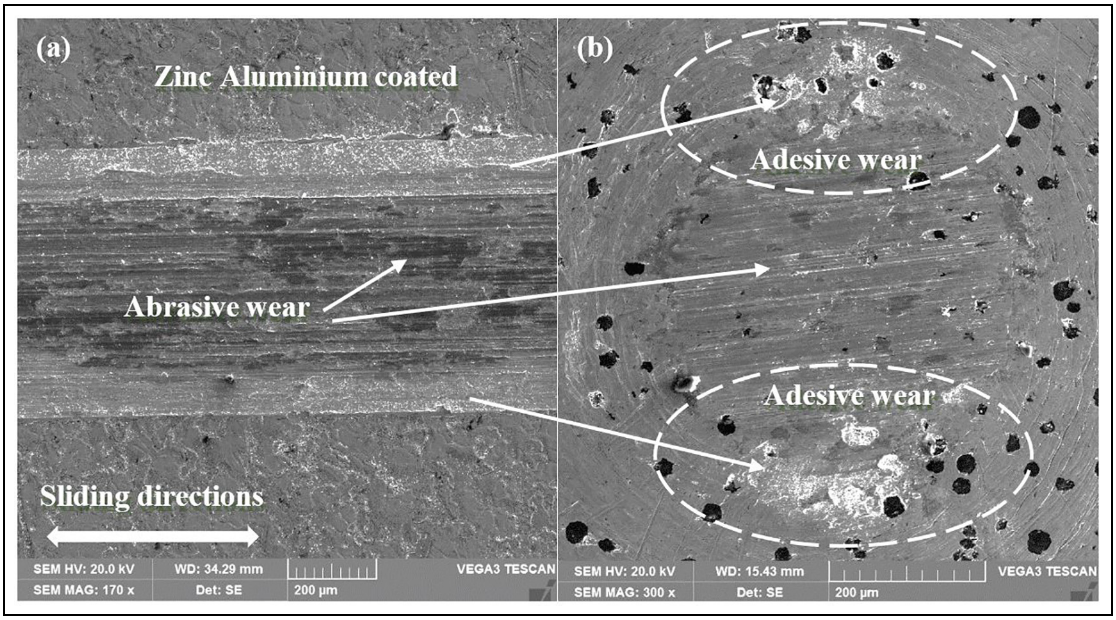

Figure 7. (a) Worn surface of the wear track of the steel plate (surface position) and (b) worn surface of the nodular cast iron pin matrix-ferrite/perlite (surface position).

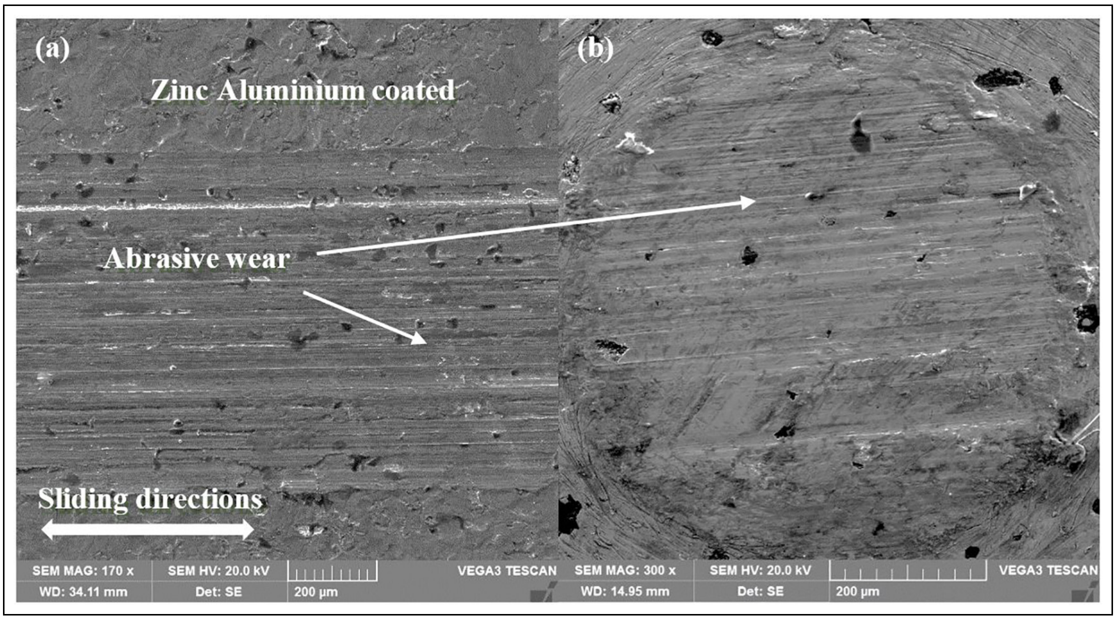

Figure 8. (a) Worn surface of the wear track of the steel plate (half radius position) and (b) worn surface of the nodular cast iron pin matrix-ferrite/pearlite (half radius position).

presents the images of the corresponding worn pins extracted from the surface, half-radius, and center of the FUCO bar, respectively. Figure 7(a) shows the SEM image of the worn surface of the steel plate wear track against the pin (surface position), Figure 7(b). The presence of longitudinal grooves along the wear tracks indicates abrasive wear mechanism with removal of material in both parts (steel plate and pin). Analyzing the pin's worn surface, some zinc/aluminum from the steel plate coating adhered to the pin's surface, characterizing adhesive wear. This type of wear mechanism is most common in low hardness materials. The high amount of ferrite (25%), which is the low hardness phase in the metal matrix of the pin (surface position), causes a higher adherence with the also low hardness zinc/aluminum coating of the plate in comparison with the half radius (HR) and the center (C) position. The half radius (HR) position, Figure 8(a) and (b), also present characteristic abrasive scratches with removal of material in both parts (steel plate and pin), but with more intense abrasive wear and with less adhesion of the steel plate coating. The center (C)

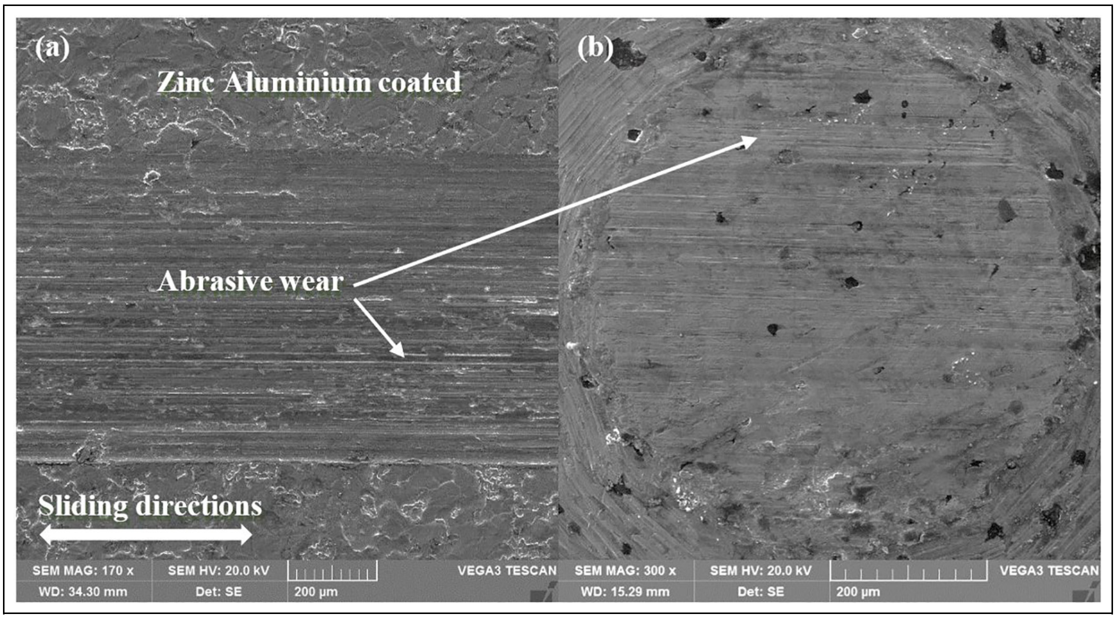

Figure 9. (a) Worn surface of the wear track of the steel plate (center position) and (b) worn surface of the nodular cast iron pin matrix-ferrite/perlite (center position).

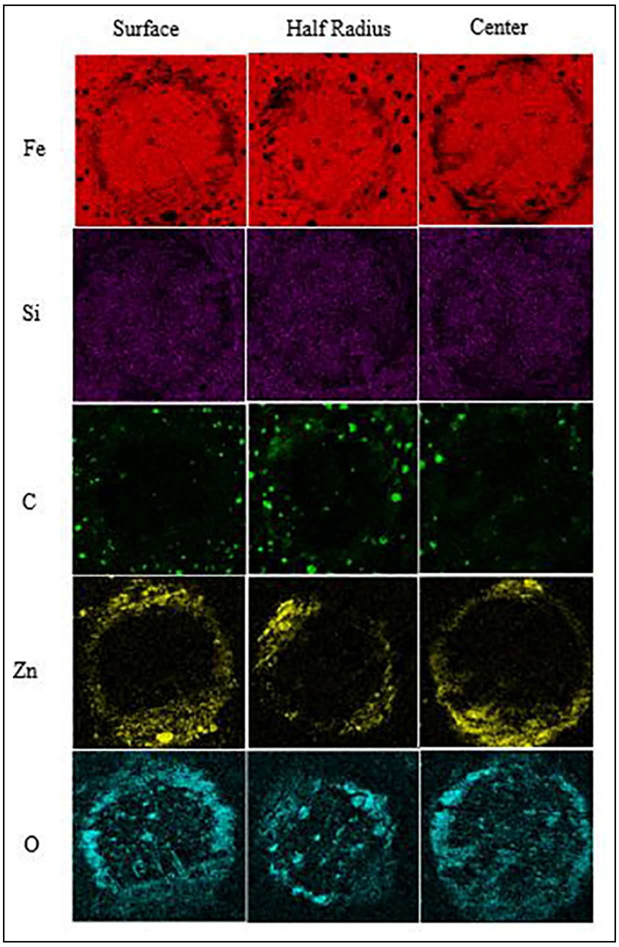

Figure 10. Chemical elemental distribution of the worn nodular cast iron pins.

position, steel bar core, which contains more pearlite and consequently greater hardness and smaller number of nodules, shows a greater intensity of abrasive wear, Figure 9(a) and (b), in both parts (plate and pin) with small amount of adhesion of the aluminum/zinc steel plate coating. During the wear test, in the center (C) position, the wear volume was higher, in consequence of the abrasive wear followed by oxidative wear. All the images reveal a similar aspect in both the steel plates and the nodular cast iron pins, exhibiting abrasive plow lines, elucidating a two-body abrasive wear mechanism affecting the steel plates.

In addition to two-body abrasive wear, the pins also exhibited adhesion of zinc, as indicated by the EDS dot maps in Figure 10. This zinc originates from the zinc-aluminum coating on the IF steel plates. Notably, zinc is found at the site of the pin shell, indicating that zinc is removed from the surface of the IF plates during the initial stages of the sliding process.

Additionally, Figure 10 shows that oxygen is present in the worn shell of the pins, indicating that there was an increase in temperature during the tribological tests. The oxidation is more significant in the pin taken from the center, which corresponds to the greater amount of pearlite illustrated in Figure 3. This suggests that the highest level of oxidative wear occurs in the pin extracted from the center of the FUCO bar.

In addition, Figure 10 also shows iron, silicon and carbon distribution; the chemical elements are primarily present in the nodular cast iron chemical composition. Silicon and iron are distributed homogeneously in the pin shell, although a depletion in iron is observed in the region where zinc is accumulated. On the other hand, carbon is concentrated in the nodules. It is possible to realize that there is a depletion of nodules in the pin shell, regardless of the position where the pin has been extracted from the FUCO bar. Figures 7(b), 8(b),

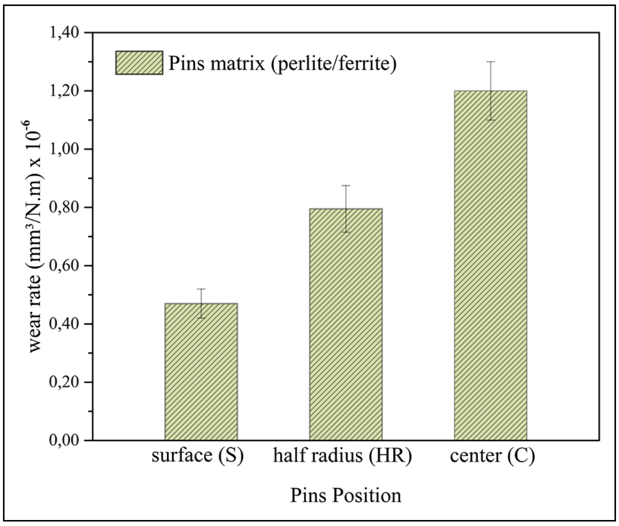

Figure 11. Wear rate of the nodular cast iron pins.

and 9(b) suggest that the graphite nodules have been removed from the pins worn shell.

Figure 11 illustrates the wear rates of nodular cast iron pins, calculated using equation 3, from the three different locations on the FUCO bar: the surface (S), half radius (HR), and center (C). The results show a significant increase in wear rate as one move from the surface toward the center position. Specifically, the pin taken from the surface exhibits a wear rate that is 65% lower than that of the pin from the center and 45% lower than that of the pin from the half radius.

A key question to consider is which microstructural feature influences the wear resistance of the pins. According to Archard's theory,[25] the wear rate is inversely related to hardness. The pin from the center, which has the highest amount of pearlite (as shown in Figure 3) and consequently the greatest hardness (as indicated in Figure 5(d)), would exhibit the lowest wear rate. However, the observation in Figure 11 shows that the hardest pin experienced the highest wear rate, suggesting that hardness alone does not fully account for wear behavior. In this case, oxidative wear more than compensate the ability of hardness to mitigate wear.

So, what is the role of graphite nodules in the wear behavior of nodular cast iron? While graphite nodules generally tend to reduce wear, the volume of nodules remains constant in the pins extracted from the three different positions of the FUCO bar, as revealed by the L/D ratio in Figure 5(c). Therefore, this microstructural factor does not explain the differences in wear behavior among the pins.

Finally, examining the tribological pair of IF steel and nodular cast iron pins, Figures 7 to 9 reveal that wear occurs in both materials. The zinc-aluminum coating is softer than the pins, so it is expected that the pins would cause wear in the IF steel. However, it is interesting to note that the coated IF steel also imposes wear on the pins. This is likely because the IF steel is a ferritic material, and since ferrite is also present in the pins and is relatively soft, it contributes to the wear of the pins as well.

Conclusions

In the first part of the investigation, it was performed a microstructural characterization of pins extracted from a FUCO bar. It was observed that a microstructural gradient developed due to the solidification rate. Specifically, as we move from the surface (S) to the center (C) of the FUCO bar, the number of graphite nodules decreases while their size increases. The ratio of the distance between two adjacent nodules to their diameter, known as the L/D ratio, remains constant. Additionally, the amount of pearlite increases while the amount of ferrite decreases as we move from the surface to the center of the FUCO bar.

In the second part of the study, pins were machined from the surface, half radius, and the center of the FUCO bar. These pins then underwent a sliding wear test against IF steel using a reciprocal mode of a tribometer. The most significant finding regarding wear behavior is that the pin with the highest amount of pearlite, which has the highest hardness, exhibited the lowest wear resistance, disagreeing with Archard's theory because oxidative wear plays a major role. The nodule features do not influence the wear behavior of the pins because their volume remains constant, according to the L/D ratio. In addition, the wear mechanism can be categorized as abrasive, followed by oxidative wear.

Declaration of conflicting interests

The author(s) declared no potential conflicts of interest with respect to the research, authorship, and/or publication of this article.

Funding

The author(s) received no financial support for the research, authorship, and/or publication of this article.

ORCID iD

Chetan P Nikhare https://orcid.org/0000-0002-2237-1350

References

1. Altan T, Lilly B and Yen YC. Manufacturing of dies and molds. *CIRP Ann* 2001; 50(2): 404–422.
2. De Souza JH and Liewald M. Analysis of the tribological behaviour of polymer composite tool materials for sheet metal forming. *Wear* 2010; 268(1–2): 241–248.
3. Pereira MP, Weiss M, Rolfe BF, et al. The effect of the die radius profile accuracy on wear in sheet metal stamping. *Int J Mach Tools Manuf* 2013; 66: 44–53.

4. Figueiredo L, Ramalho A, Oliveira MC, et al. Experimental study of friction in sheet metal forming. *Wear* 2011; 271(9–10): 1651–1657.
5. Pereira MP, Yan W and Rolfe BF. Wear at the die radius in sheet metal stamping. *Wear* 2012; 274: 355–367.
6. Kirkhorn L, Bushlya V, Andersson M, et al. The influence of tool steel microstructure on friction in sheet metal forming. *Wear* 2013; 302(1–2): 1268–1278.
7. Masen MA. *Abrasive tool wear in metal forming processes*. PhD Thesis, University of Twente, Enschede, The Netherlands, 2004.
8. Hase A. Visualization of the tribological behavior of graphite in cast iron by in situ observations of sliding interfaces. *Tribol Int* 2019;138: 40–46.
9. Behnam MJ, Davami P and Varahram N. Effect of cooling rate on microstructure and mechanical properties of gray cast iron. *Mater Sci Eng A* 2010; 528(2): 583–588.
10. Rebasa N, Dommarco R and Sikora J. Wear resistance of high nodule count ductile iron. *Wear* 2002; 253(7–8): 855–861.
11. Abedi HR, Fareghi A, Saghafian H, et al. Sliding wear behavior of a ferritic–pearlitic ductile cast iron with different nodule count. *Wear* 2010; 268(3–4): 622–628.
12. Liu C, Du Y, Wang X, et al. Comparison of the tribological behavior of quench-tempered ductile iron and austempered ductile iron with similar hardness. *Wear* 2023; 520: 204668.
13. Turu IC and Gecu R. Wear and corrosion behavior of vanadium-alloyed nodular cast irons fabricated by sand-casting. *Wear* 2023; 534: 205143.
14. Shin WS, Baek S and Kim YJ. Effect of Sn addition on the microstructure and friction–wear properties of a nodular graphite cast iron. *Kor J Metals Mater* 2022; 60(6): 471–477.
15. Baron C, Stawarz M, Studnicki A, et al. Abrasive wear resistance of nodular cast iron after selected surface heat and thermochemical treatment processes. *Arch Foundry Eng* 2024; 4(3): 25–35.
16. Oktadinata H, Pratomo SB, Dwiwanto SA, et al. Microstructural investigation of acicular nodular cast iron used for work rolls. *Mater Sci Forum* 2022; 1067: 47–52.
17. Tkaya MB, Mezlini S, El Mansori M, et al. On some tribological effects of graphite nodules in wear mechanism of SG cast iron: finite element and experimental analysis. *Wear* 2009; 267(1–4): 535–539.
18. Qiu Y, Pang JC, Li SX, et al. Influence of thermal exposure on microstructure evolution and tensile fracture behaviors of compacted graphite iron. *Mater Sci Eng A* 2016; 664: 75–85.
19. Groche P, Moeller N, Hoffmann H, et al. Influence of gliding speed and contact pressure on the wear of forming tools. *Wear* 2011; 271(9–10): 2570–2578.
20. Voss BM, Pereira MP, Rolfe BF, et al. A new methodology for measuring galling wear severity in high strength steels. *Wear* 2017; 390: 334–345.
21. Zhao H, Li J, Zheng Z, et al. The microstructures and tribological properties of composite coatings formed via PTA surface alloying of copper on nodular cast iron. *Surf Coat Technol* 2016; 286: 303–312.
22. Fernandes L, Silva FJ, Andrade MF, et al. Improving the punch and die wear behavior in tin coated steel stamping process. *Surf Coat Technol* 2017; 332: 174–189.
23. Da Silva LR, Del Claro VT, Andrade CL, et al. Tool wear monitoring in drilling of high-strength compacted graphite cast irons. *Proc IMechE, Part B: J Engineering Manufacture* 2021; 235(1–2): 207–218.
24. Al Bahkali EA, Ragab AE, El Danaf EA, et al. An investigation of optimum cutting conditions in turning nodular cast iron using carbide inserts with different nose radius. *Proc IMechE, Part B: J Engineering Manufacture* 2016; 230(9): 1584–1591.
25. Buchner S, Mikowski A, Lepienski CM, et al. Mechanical and tribological properties of a sintered glass-ceramic compared to granite and porcelainized stoneware. *Wear* 2011; 271(5–6): 875–880.